Available online at www.sciencedirect.com

SCIENCE DIRECT®

Journal of Molecular Catalysis A: Chemical 204–205 (2003) 693–701

JOURNAL OF MOLECULAR CATALYSIS A: CHEMICAL

www.elsevier.com/locate/molcata

Adsorption and photocatalytic degradation of acetonitrile: FT-IR investigation

P. Davit [a,*], G. Martra [a], S. Coluccia [a], V. Augugliaro [b], E. García López [b], V. Loddo [b], G. Marcì [b], L. Palmisano [b], M. Schiavello [b]

[a] *Dipartimento di Chimica IFM, Università di Torino, Via Pietro Giuria 7, I-10125 Torino, Italy*
[b] *Dipartimento di ICPM, Università di Palermo, Viale delle Scienze, 90128 Palermo, Italy*

Received 22 October 2002; received in revised form 30 January 2003; accepted 14 February 2003

Dedicated to Professor Renato Ugo on the occasion of his 65th birthday

Abstract

The photocatalytic degradation of acetonitrile was carried out in liquid–solid regime in a batch reactor by using two types of commercial TiO_2 powders (Merck and Degussa P25) as photocatalysts. The concentration of acetonitrile and non-purgeable organic carbon (NPOC) were monitored. The initial rate of acetonitrile conversion was found higher on TiO_2 Merck than on TiO_2 P25.

FT-IR spectroscopy was used to investigate the molecular features of the adsorption and photo-oxidation of acetonitrile on the two TiO_2 powders in a fully surface hydrated form. Acetonitrile was found adsorbed on Ti^{4+} surface ions and hydroxyl groups for both types of TiO_2. This interaction appeared fully reversible in the case of the Merck photocatalyst, whereas acetonitrile was more strongly stabilized on Ti^{4+} ions of TiO_2 P25. Furthermore, the adsorption of $CD_3CN\cdots Ti^{4+}$ on this type of photocatalyst resulted in the formation of acetamide-like species, because of the presence of nucleophilic surface O^{2-} and hydroxyl groups. The formation of these species, strongly bound to the TiO_2 surface and recalcitrant to the photo-oxidation, could result in the poisoning of a part of the photocatalytic sites of TiO_2 P25, accounting for its lower initial acetonitrile conversion rate.

Keywords: TiO_2; Acetonitrile; Adsorption; Photocatalysis; FT-IR investigation

1. Introduction

Acetonitrile is a widely used molecular probe for the characterization of Lewis and Brønsted acid sites, through the interaction with the electron lone-pair located on the nitrogen atom, which causes a high frequency shift of the stretching ν(CN) mode with respect to the liquid phase. This is due to the strengthening of the CN bond caused by the rehybridization of the nitrogen orbitals, leading to an increase of the strength of the σ-bond component [1]. The shift of the ν(CN) mode increases with the acidity of the centers involved.

Moreover, the ν(CN) mode of the free CH_3CN molecule is affected by a Fermi resonance with the $\delta_S(CH_3) + \nu(CC)$ combination [2] which perturbs the determination of the ν(CN) shift in complexes or interacting with surface sites. Therefore CD_3CN is

* Corresponding author. Tel.: +39-011-6707536; fax: +39-011-6707855.
E-mail address: patrizia.davit@unito.it (P. Davit).

1381-1169/$ – see front matter © 2003 Elsevier Science B.V. All rights reserved.
doi:10.1016/S1381-1169(03)00354-6

frequently used instead of CH_3CN since in this case the ν(CN) is not perturbed.

On the other hand, in the presence of basic O^{2-} anions, acetonitrile may act as a Brønsted acid. Hydrogen atoms of the CH_3 group in α-position to the CN bond show a proton donor character and may lead to the CH_2CN^- anion by the rupture of a C–H bond. Therefore, owing to its acid and basic character, acetonitrile is a very sensitive probe to study the surface properties of metal oxides.

Acetonitrile can also undergo an hydrolytic process, reacting with the hydroxyl groups on the surface of the oxide, giving rise first to acetamide-like species [3,4] and then to acetic acid and ammonia, as observed in homogeneous catalysis.

Moreover, acetonitrile is an interesting molecule for photo-oxidation studies, since its alkyl and cyanide groups may undergo different degradation pathways. In addition, the CN moiety is representative of several toxic materials which are good candidates for TiO_2-based solar driven photocatalytic studies.

Litchin and Avudaithai [5] reported the feasibility of the photocatalytic oxidation of acetonitrile both in liquid and in vapor phase, in the presence of O_2 as an oxidant. They found cyanogen $(CN)_2$ as an intermediate species, indicating the formation of $CN^{\bullet}$ radicals which can dimerize. Acetonitrile showed to be much more reactive in gas phase than in liquid phase. Zhuang et al. [6] have recently reported photo-oxidation of acetonitrile adsorbed on TiO_2, and investigated the reaction mechanism by means of infrared spectroscopy. The final oxidation products in the presence of O_2 were CO_2 and H_2O, but also CNO^- was found as a partially oxidized species adsorbed onto the surface.

The photocatalytic oxidation of acetonitrile carried out in aqueous suspensions of polycrystalline TiO_2 P25 Degussa irradiated by sunlight has been also reported [7]. A plug flow photoreactor in a total recycle loop was used and concentrations of acetonitrile, intermediate products and non-purgeable organic carbon (NPOC) were monitored. First order kinetics well fit the data with respect to acetonitrile and NPOC concentrations and total abatement of acetonitrile both in the absence and in the presence of strong oxidant species (H_2O_2, $S_2O_8{}^{2-}$, ClO^-) is reported. The presence of cyanate is a strong clue to the formation of cyanide species and, indeed, previous studies showed that the main oxidation products of free [8,9] and complex cyanides [10] were cyanate, nitrite, nitrate and carbonate/hydrogen carbonate ions.

The aim of the present investigation is the study of the photocatalytic degradation of acetonitrile in aqueous TiO_2 dispersion irradiated by near-UV light. The kinetics of the photocatalytic process were investigated for two commercial TiO_2 powders (Merck and Degussa P25).

Moreover, an investigation of the phenomena occurring during acetonitrile adsorption and photo-oxidation on the TiO_2 surface was carried out by FT-IR spectroscopy simulating the experimental conditions used for the photoreaction. In particular, the attention was focused on the study of the interaction between acetonitrile and the TiO_2 surface, with the aim of understanding the molecular mechanisms occurring during the process.

2. Experimental

2.1. Photoreactivity set-up, catalysts and analytical procedures in liquid–solid regime

For the reactivity experiments in the liquid–solid system, a Pyrex batch photoreactor of cylindrical shape containing 1.5 l of aqueous suspension was used. The photoreactor was provided with ports in its upper section for the inlet and outlet of gases, for sampling and for pH and temperature measurements. A 500 W medium pressure Hg lamp (Helios Italquartz, Italy) was immersed within the photoreactor.

The photon flux emitted by the lamp was measured using a radiometer (UVX Digital) leaned against the external wall of the photoreactor containing only pure water. The mean value of the radiation power impinging on the photoreactor was 16.3 mW cm^{-2}. Oxygen was continuously bubbled into the suspension for ca. 0.5 h before switching on the lamp and throughout the occurrence of the photoreactivity experiments.

The photocatalysts used for the experiments were commercial polycrystalline TiO_2 Merck (100% anatase, $SSA_{BET} = 10\,m^2\,g^{-1}$), and Degussa P25 (80% anatase and 20% rutile, $SSA_{BET} = 50\,m^2\,g^{-1}$).

The amount of catalyst used for the experiments was 0.4 g l^{-1}, and the initial acetonitrile concentration ranged between 0.24 and 2.2 mM. 0.4 g l^{-1} of catalyst were sufficient to absorb almost all the photons

Table 1
Initial reaction rate (r_0), initial reaction rate per square meter (r'_0) of photocatalyst and quantum efficiency (η) for acetonitrile disappearance at different initial concentrations

TiO_2	$C_0(CH_3CN)$ (mM)	r_0 ($\times 10^8$ M s^{-1})	r'_0 ($\times 10^8$ M s^{-1} m^{-2})	η (%)
P25	0.24	3.7	0.12	0.18
P25	0.50	3.8	0.13	0.19
P25	1.2	4.3	0.14	0.22
P25	2.2	4.3	0.14	0.22
Merck	0.24	3.8	0.63	0.19
Merck	0.50	5.3	0.88	0.27
Merck	1.2	7.0	1.16	0.35
Merck	2.2	5.8	0.96	0.29

emitted by the lamp, as verified by using the radiometer. The initial pH of the suspension was adjusted at 11 by adding NaOH (Merck). The temperature inside the reactor was ca. 300 K. Moreover, in order to determine quantum efficiency (η), reported in Table 1, the ferrioxalate actinometer method was used for measuring the photon flow inside the photoreactor [11]. The absorbance of the actinometer solution was measured at 510 nm. The value of the photon flow was 1.99×10^{-5} einstein s^{-1} l^{-1}.

The photoreactivity runs lasted 6.0 h including the first half hour during which the lamp was switched-off. Samples of 5 ml volume were withdrawn from the suspensions every 30 or 60 min for analyses and the catalysts were separated from the solution by filtration through 0.45 mm cellulose acetate membranes (HA, Millipore).

The quantitative determination of CH_3CN was routinely performed by using a gas chromatograph (Hewlett-Packard, GC 6890 system) equipped with a column (Hewlett-Packard HP-1) and a FID detector. Chromatographic grade helium was used as carrier gas. The sample was placed in a vial and the compounds present in the vapor phase were extracted (extraction time, 5 min) by using a 75 μm Carboxen-PDMS solid phase micro-extraction (SPME) fiber assembly (Supelco) with a fiber holder for manual sampling. Then the holder was placed in the split/splitless injector, maintained at a temperature of 250 °C for 2 min before starting the analysis. The temperature of the oven was held at 40 °C for the first 3 min, then it was increased up to 250 °C at a rate of 60 °C min^{-1}.

The quantitative determination of ionic species was carried out by using an ionic chromatograph system (Dionex DX 120) equipped with an Ion Pac AS14 4 mm column (250 mm long, Dionex). Aqueous solutions of $NaHCO_3$ (Merck) (1 mM) and Na_2CO_3 (Merck) (3.5 mM) were used as eluants at a flow rate of 1.67×10^{-2} cm^3 s^{-1}. A 5000A Shimadzu total organic carbon analyzer was used in order to determine the NPOC content of the samples.

2.2. FT-IR apparatus and procedures

TiO_2 powders were pressed in the form of self-supporting pellets (ca. 20 mg cm^{-2}) and put in a conventional IR quartz cell equipped with CaF_2 windows connected to a vacuum line (residual pressure: 1×10^{-6} Torr, 1 Torr = 133.33 Pa) which allowed adsorption–desorption experiments to be carried out in situ.

For the reason reported in the Introduction, CD_3CN (99.8%, Aldrich), was employed. In order to avoid any exchange of the deuterium atoms of CD_3CN with the hydrogen atoms of the hydroxyl groups and water molecules present on the surface of the photocatalysts, the TiO_2 pellets were submitted to several D_2O (99.9%, Aldrich) vapor adsorption–desorption cycles and finally outgassed at room temperature prior to contact with acetonitrile. The accomplishment of the OH/OD and H_2O/D_2O exchange was monitored by IR spectroscopy.

The FT-IR spectra (4 cm^{-1} resolution) of the TiO_2 pellets were recorded with a Bruker Vector 22 spectrophotometer equipped with a MCT detector.

In the photo-oxidation experiments the TiO_2 pellets were irradiated in presence of O_2 (100 Torr; high purity, Praxair) and D_2O (18 Torr) through the quartz walls of the IR cell by the same type of lamp employed for the catalytic tests, equipped with a Pyrex filter.

3. Results and discussion

3.1. Photoreactivity results

Some preliminary experiments have been carried out in order to investigate the adsorption of acetonitrile onto the catalyst surface. Acetonitrile concentrations of the liquid phase were measured before and after the addition of TiO_2 powder. The acetonitrile values did not show a significant difference with respect to that of the starting solution even after long times of contact. The conclusion was drawn that acetonitrile scarcely adsorbs in the dark onto the TiO_2 surface. It is worth noting that photo-adsorption and photo-desorption phenomena on the catalyst surface can occur during the irradiation of the suspension, but it is difficult to quantify them due to the fact that these phenomena take place contemporarily to photodegradation.

Fig. 1 reports acetonitrile concentration versus irradiation time for two selected experiments carried out by using TiO_2 Degussa P25 (a) and TiO_2 Merck (b). It can be observed that the initial reaction rate of acetonitrile disappearance is higher by using TiO_2 Merck than by using TiO_2 Degussa P25.

Table 1 reports initial reaction rate (r_0), initial reaction rate per square meter (r_0') of photocatalyst and quantum efficiencies (η) for acetonitrile disappearance at different initial concentrations. In Fig. 2, the r_0' values versus different initial concentrations of acetonitrile in the liquid phase are plotted. It can be observed that the initial reaction rates r_0' are ca. 5–8 times higher for TiO_2 Merck than for TiO_2 Degussa P25, and TiO_2 Merck showed to be more photo-active also when the r_0 values are compared.

The values reported in Table 1 are mean values obtained by considering three different experiments. Each value of r_0 was obtained by applying a least-square fitting procedure to the experimental data and the differences between the three figures obtained in this way ranged between 1 and 4%.

Moreover, it has been observed that acetonitrile can be photocatalytically oxidized until complete mineralization by using both types of catalysts.

For both catalysts the almost complete mineralization of the substrate was achieved after similar reaction times (ca. 25 h), while the disappearance of the substrate was almost complete after ca. 5 h, for the lowest concentrations.

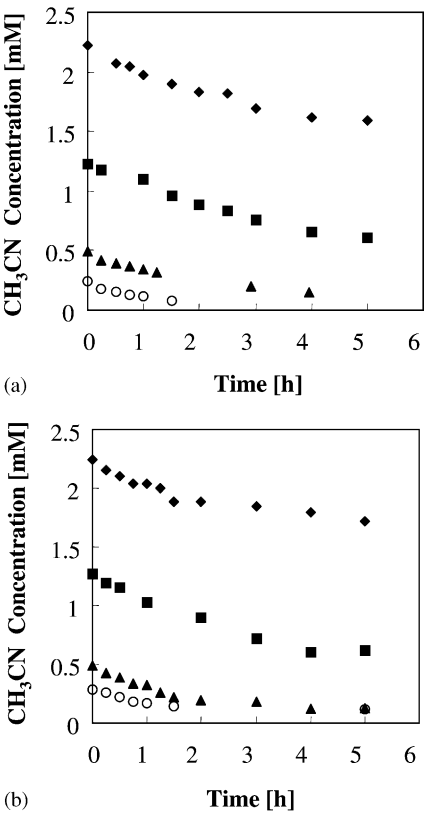

Fig. 1. Acetonitrile concentration versus irradiation time for runs carried in the liquid–solid system by using as photocatalysts: (a) TiO_2 Degussa P25 and (b) TiO_2 Merck.

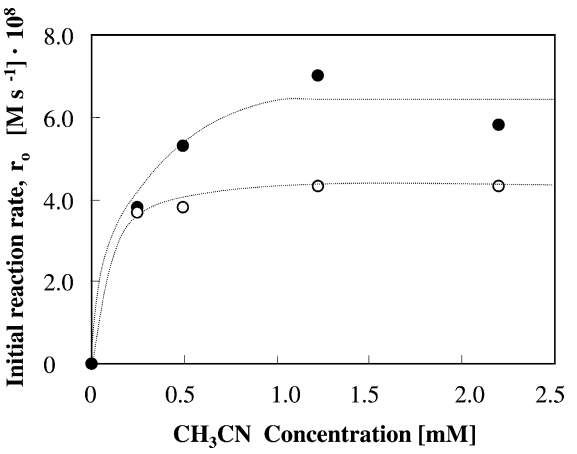

Fig. 2. Initial reaction rate per square meter of catalysts vs. initial acetonitrile concentration for runs carried in the liquid–solid system by using as photocatalysts: (○) TiO_2 Degussa P25 and (●) TiO_2 Merck.

The lower photoactivity of TiO_2 Degussa P25 with respect to TiO_2 Merck and the fact that the initial reaction rates for Degussa P25 does not change significantly by increasing the initial concentration of acetonitrile, indicating a plateau of acetonitrile coverage on the surface, suggests the formation of some stable intermediate species which remain strongly adsorbed onto the catalyst surface and de-activate part of the catalytic sites.

3.2. FT-IR investigation

In order to understand the molecular phenomena involved in the process on the TiO_2 surface and to explain the differences in the photo-activity observed for the two TiO_2 powders, acetonitrile adsorption and photo-oxidation were studied by FT-IR spectroscopy.

Although two crystallographic phases (anatase 80%, rutile 20%) have been recognized in the bulk structure of TiO_2 Degussa P25 particles, their surface structure has been found to correspond to that of anatase phase [12–14]. Thus, it seems reasonable to compare the behavior of TiO_2 Degussa P25 and TiO_2 Merck towards acetonitrile in terms of differences of anatase surface faces depending on the particle morphology, as stated in previous studies [15].

The acetonitrile adsorption was carried out on the photocatalysts simply outgassed at room temperature. In this condition the TiO_2 surface is still completely covered with a full monolayer of hydroxyl groups and coordinated water molecules, as should occur in the first interface layer at the solid/liquid boundary in the photocatalytic experiments carried out with TiO_2 in aqueous suspension.

The FT-IR spectra related to the adsorption of acetonitrile are reported in Figs. 3 and 4 for TiO_2 Merck and TiO_2 Degussa P25, respectively.

The spectrum of the TiO_2 Merck pre-outgassed at room temperature after isotopic exchange (OH/OD: H_2O/D_2O) (Fig. 3, curve a) exhibits an asymmetric peak at 2670 cm^{-1}, with a broad shoulder at 2707 cm^{-1}, and a very broad absorption in the 2650–2200 cm^{-1}. At lower frequency, a complex pattern of weak bands is observed in the range 1800–1300 cm^{-1}. The components at higher wavenumbers can be assigned to the stretching mode of isolated deuteroxyl groups, while the broad band in the 2650–2200 cm^{-1} range results from the overlap of

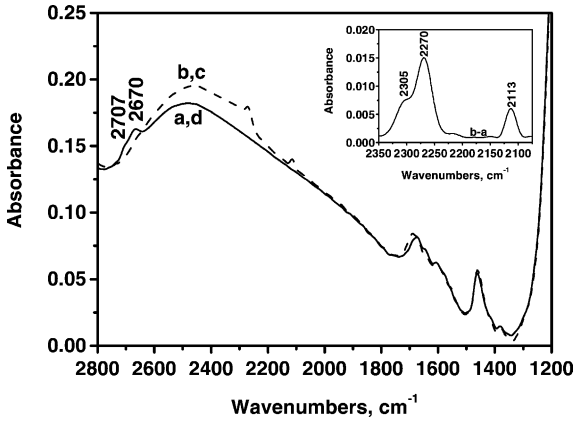

Fig. 3. FT-IR absorbance spectra (recorded using the IR lamp as a background) of TiO_2 Merck: (a) outgassed at room temperature, (b) after the admission of 5 mbar of CD_3CN, (c) after 45 min contact with CD_3CN and (d) subsequently outgassing at room temperature for 10 min. Inset: FT-IR absorbance spectra (recorded using the sample outgassed at room temperature as a background) of TiO_2 Merck after the admission of 5 mbar of CD_3CN.

the bands due to the stretching mode of D-bonded OD groups and of D_2O molecules coordinated to surface Ti^{4+} cations [16]. The bands in the 1800–1300 cm^{-1} range are due to carbonate-like species [17].

By admitting acetonitrile onto the sample (Fig. 3, curve b), the peak at 2670 cm^{-1} and its shoulder at 2707 cm^{-1} completely disappear, being converted into a broad component superimposed to the absorption

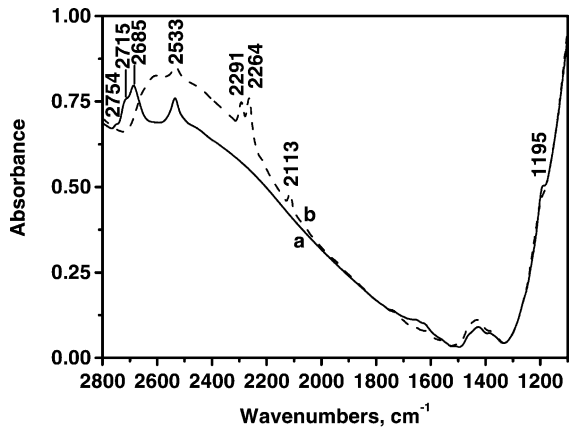

Fig. 4. FT-IR absorbance spectra (recorded using the IR lamp as a background) of TiO_2 Degussa P25: (a) outgassed at room temperature and (b) after the admission of CD_3CN vapor pressure (≈100 Torr).

in the 2650–2200 cm^{-1} range. This behavior monitors the occurrence of a D-bonding between isolated deuteroxyl groups and CD_3CN molecules, interacting with the OD through their lone-pair on the nitrogen atom. On the other hand, weak bands due to adsorbed acetonitrile appear at 2270 and 2113 cm^{-1}. The adsorption of CD_3CN molecules seems also to perturb in some extent the carbonate-like groups present on the TiO_2 surface, as their bands in the 1800–1300 cm^{-1} range appear slightly modified. A clearer view of the bands due to adsorbed CD_3CN is reported in the inset of Fig. 3, where the spectrum resulting from the subtraction of curve a from curve b in the main frame is shown. The main component at 2270 cm^{-1} is due to the ν(CN) mode of acetonitrile molecules D-bonded to surface deuterated hydroxyl groups. The relatively small shift of the peak with respect to the ν(CN) mode of liquid CD_3CN (2262 cm^{-1} [1] and reference therein) indicates that this interaction is quite weak.

The shoulder at 2305 cm^{-1} corresponds to the ν(CN) mode of CD_3CN adsorbed on stronger Lewis acid sites. This interaction could result from the displacement by acetonitrile of D_2O molecules coordinated to surface Ti^{4+} cations. Unfortunately, the band due to the deformation mode of these D_2O molecules, which should be sensitive to such ligand-displacement effect, expected at ca. 1200 cm^{-1}, falls at a frequency lower than the cut-off of TiO_2 Merck (ca. 1250 cm^{-1}). However, a confirmatory evidence of this proposed displacement was observed in the case of TiO_2 Degussa P25 (see below).

Finally, the weaker component at 2113 cm^{-1} corresponds to the symmetric $\nu(CD_3)$ mode, which is less sensitive to the coordination of CD_3CN to surface centers. Other CD_3CN bands expected below 2000 cm^{-1} are apparently too weak to be detected.

No changes were observed by increasing the time of contact with acetonitrile (Fig. 3, curve c). Moreover, all CD_3CN bands disappear by outgassing at room temperature and the peaks due to the isolated deuteroxyl groups are restored (Fig. 3, curve d), indicating the complete desorption of the weakly adsorbed species.

The spectrum of the TiO_2 Degussa P25 pre-outgassed at room temperature (Fig. 4, curve a) exhibits an asymmetric peak at 2685 cm^{-1} with two shoulders at higher wavenumbers (2715 and 2754 cm^{-1}), indicating a greater heterogeneity of isolated OD groups with respect to the Merck catalyst, while the peak at 2533 cm^{-1} is due to the stretching mode of D_2O molecules coordinated to Ti^{4+} sites. As in the case of the TiO_2 Merck, the spectroscopic pattern in the 1800–1300 cm^{-1} range reveals the presence of carbonate-like species. In the case of TiO_2 P25 Degussa, which exhibits the cut-off at ca. 1150 cm^{-1}, a weak band at 1195 cm^{-1}, due to the deformation mode of D_2O molecules coordinated to surface Ti^{4+} ions, is observed.

By admitting acetonitrile onto the sample, the peak at 2685 cm^{-1} and its shoulders disappear and are transformed into a broad absorption in the range 2750–2200 cm^{-1} (Fig. 4, curve b) revealing the formation of D-bonding between OD groups and the N lone-pair of CD_3CN molecules. In the 2300–2000 cm^{-1} range peaks at 2291 and 2264 cm^{-1} (ν(CN)) and at 2113 cm^{-1} ($\nu_{sym}(CD_3)$) due to adsorbed acetonitrile appear, and a slight modification of the carbonate-like pattern in the 1800–1300 cm^{-1} range occurs. Noticeably, the band at 1195 cm^{-1} due to D_2O molecules coordinated to surface Ti^{4+} ions is converted in a very weak absorption at higher frequency. This behavior clearly monitors the occurrence of a ligand displacement of D_2O molecules from surface Ti^{4+} cations by CD_3CN. Acetonitrile molecules adsorbed on such sites are responsible for the ν(CN) band at 2291 cm^{-1}, while the peak at 2264 cm^{-1} is due to the ν(CN) of CD_3CN in weaker interaction with OD groups. Finally, as reported above, the 2113 cm^{-1} weaker component is common to acetonitrile molecules adsorbed in both forms. Furthermore, additional experiments carried out by admitting D_2O on the sample with pre-adsorbed acetonitrile, reveals that also CD_3CN molecules adsorbed on Ti^{4+} ions, but surrounded by water molecules, partly contribute to the 2264 cm^{-1} peak (spectra not reported).

Differently from what observed for TiO_2 Merck, a significant evolution of the spectral pattern of the adsorbed species was observed by increasing the time of contact. For the sake of clarity, the spectra obtained are reported having subtracted the spectrum of the sample before acetonitrile adsorption (Fig. 5). In this form, positive bands are due to adsorbed species, while the negative band at 1195 cm^{-1} corresponds to the D_2O initially coordinated to Ti^{4+} ions and then displaced by CD_3CN molecules.

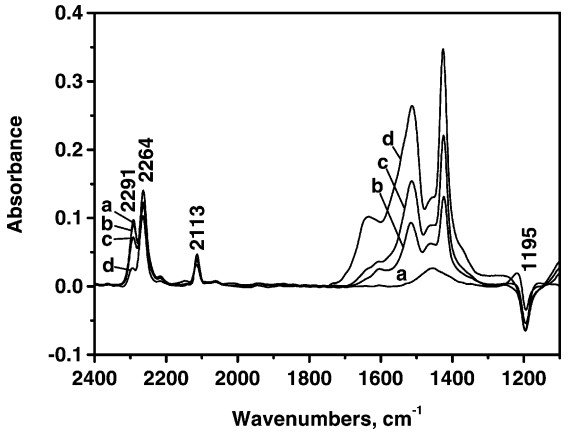

Fig. 5. FT-IR absorbance spectra (recorded using the sample outgassed at room temperature as a background) of TiO_2 Degussa P25: (a) after the admission of CD_3CN vapor pressure (≈100 Torr), (b) after 1 h contact with CD_3CN, (c) after 3 h contact with CD_3CN and (d) after 12 h contact with CD_3CN.

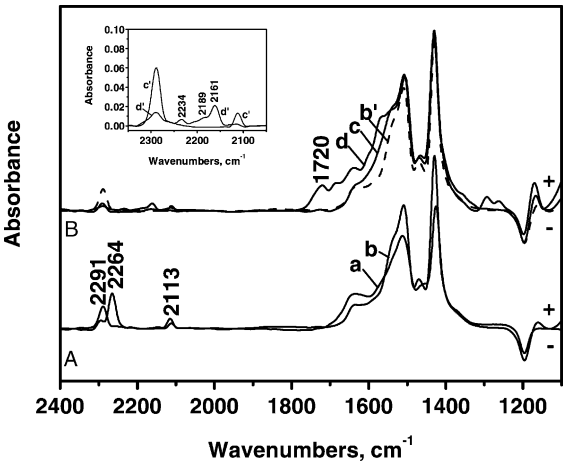

Fig. 6. Section A: FT-IR absorbance spectra (recorded using the sample outgassed at room temperature as a background) of (a) CD_3CN adsorbed on TiO_2 Degussa P25, after 12 h contact with CD_3CN, (b) after outgassing CD_3CN for 45 min. Section B: (b′) the same as (b), (c) after 2 h UV irradiation in presence of O_2 and D_2O and subsequent outgassing of O_2 and D_2O and (d) after 17 h UV irradiation in presence of O_2 and D_2O and subsequent outgassing of O_2 and D_2O. Inset: (c′) the same as (c) and (d′) the same as (d).

In the 2300–2000 cm^{-1} range, a decrease of the intensity of all peaks is observed, particularly evident for the signal at 2291 cm^{-1}. Moreover, a complex pattern in the range 1700–1350 cm^{-1} appears and evolves by increasing the contact time. Similar spectroscopic features have been previously reported, for example, for CeO_2 [3], ZrO_2 [4] and ZnO [18], and related to the formation of acetamide-like species by reaction of adsorbed acetonitrile molecules with surface basic centers. In the present case, the observed spectral behavior indicates that acetonitrile molecules initially adsorbed on Ti^{4+} cations react with adjacent O^{2-} anions (or OD groups), which in the case of Degussa P25 are basic enough [15] to give a nucleophilic attack to CD_3CN forming acetamide-like species.

For the mechanism of the formation of such species on ZrO_2, a scheme of the process was proposed [4]. Such mechanism may tentatively be invoked to occur at the surface of the TiO_2 Degussa P25, in the presence of D_2O molecules displaced from Ti^{4+} sites by CD_3CN (Scheme 1).

A subsequent outgassing at room temperature affected to some extent the bands of surface species (Fig. 6A, curves a and b). The peak at 2264 cm^{-1} disappears, mainly as a consequence of the desorption of acetonitrile molecules from surface OD groups (the stretching bands of which, falling in the 2750–2650 cm^{-1} range, are fully restored; spectra not reported). The desorption of such molecules is responsible for the decrease in intensity of the weaker

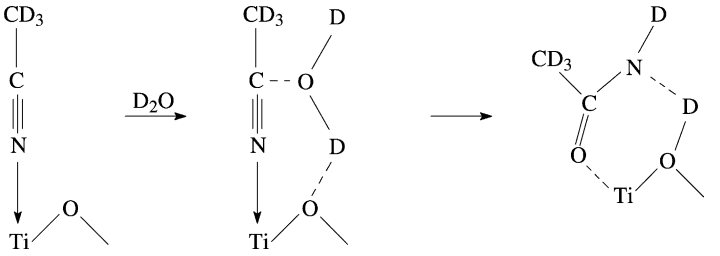

Scheme 1.

component at 2113 cm^{-1}. The outgassing resulted also in the removal of D_2O "solvating" part of CD_3CN molecules coordinated to Ti^{4+} ions (contributing, when in such form, to the 2264 cm^{-1} peak), which are converted in new "dehydrated" adducts, responsible for the increase in intensity of the 2291 cm^{-1} band. This band appears irreversible by outgassing at room temperature, indicating a higher stability of the $CD_3CN \cdots Ti^{4+}$ adducts with respect to the corresponding species formed on TiO_2 Merck. Conversely, its location at a wavenumbers (2291 cm^{-1}) lower than that observed for $CD_3CN \cdots Ti^{4+}$ species on TiO_2 Merck (2305 cm^{-1}) could suggest a weaker interaction of acetonitrile molecules with Ti^{4+} ions (see Section 1). As previously reported for the adsorption of CD_3CN on MgO [19], a small shift of the ν(CN) band of adsorbed acetonitrile molecules combined with an increase of the strength of adsorption results from their interaction with multiple cationic sites located in defect positions.

The presence of the spectral pattern of acetamide-like species in the 1750–1350 cm^{-1} range after outgassing indicates that these species are irreversibly adsorbed on the surface of the photocatalyst. The observed changes in their feature can be related to the occurrence of some modification in the structure of such surface species by desorption of D_2O and physisorbed CD_3CN molecules.

After outgassing, UV irradiation for increasing time in the presence of O_2 and D_2O was carried out. At the end of each irradiation step, O_2 and D_2O were outgassed, and the IR spectrum of the sample was recorded. The results are reported in Fig. 6B, curves c and d (curve b′ corresponds to curve b in Fig. 6A, and is reported for sake of clarity).

By irradiation for 2 h, a decrease in intensity of the band at 2291 cm^{-1} is observed, accompanied by a growth of the absorptions in the 1750–1350 cm^{-1} range (Fig. 6B, curve c), monitoring the occurrence of a photostimulated conversion of CD_3CN adsorbed on Ti^{4+} ions in acetamide-like adducts. For UV irradiation up to 17 h (Fig. 6B, curve d), the peaks due to acetamide-like adducts appear almost unchanged, while the weak band at 2291 cm^{-1} due to residual $CD_3CN \cdots Ti^{4+}$ species considerably decreases in intensity (Fig. 6B, inset). On the other hand, new components appear, assignable to cyanate (2234 cm^{-1}) [20], isocyanate (2189 cm^{-1}) [21], formyl (1720 cm^{-1}) [22], carbonate and bicarbonate (1700–1450 cm^{-1} range) [15,17] and nitrate (1560–1500 cm^{-1} and 1300–1250 cm^{-1} ranges) [23] species, which result from the photo-oxidation of CD_3CN coordinated to Ti^{4+} ions. Moreover, the weak band at 2161 cm^{-1} is likely due to polymerized CD_3CN [4].

This behavior indicates that acetamide-like species are less sensitive to the photo-oxidation than acetonitrile adsorbed in molecular form. Thus, these species can exhibit a poisoning effect towards part of the photocatalytic surface sites, accounting for the lower initial reaction rate observed for TiO_2 Degussa P25 with respect to TiO_2 Merck.

4. Conclusions

In the adopted liquid–solid regime, the photo-oxidation of acetonitrile occurs until complete mineralization on both types of TiO_2 powders (Merck and Degussa P25) considered, but with a significantly higher initial rate for the TiO_2 Merck photocatalyst.

FT-IR investigations indicates that acetonitrile is adsorbed on both type of TiO_2 by interaction between the nitrogen lone-pair and TiO_2 Lewis acid sites (Ti^{4+} surface cations and deuteroxyl groups). This interaction is very weak in the case of the Merck catalyst, and it is completely reversible by simply outgassing the sample at room temperature. Conversely, in the case of TiO_2 Degussa P25 acetonitrile is more strongly stabilized on Ti^{4+} ions, and part of the $CD_3CN \cdots Ti^{4+}$ adducts are converted, even in the absence of UV light, in acetamide-like species by nucleophilic attack of basic surface O^{2-} and hydroxyl groups.

These species are strongly bound to the TiO_2 surface and scarcely sensitive to the photo-oxidation. Thus, they can persist on the photocatalyst for long time, and act as poisoning species of a part of the photocatalytic sites. This could account for the lower initial conversion rate of acetonitrile obtained by using TiO_2 Degussa P25.

Acknowledgements

This work has been carried out in the framework of the Consorzio Interuniversitario Nazionale "La Chimica per l'Ambiente"—INCA. The authors wish

to thank the “Ministero dell’Istruzione, Università e Ricerca” (MIUR) for financial support.

References

[1] E. Escalona Platero, M. Peñarroya Mentruit, C. Morterra, Langmuir 15 (1999) 5079.
[2] H. Knözinger, H. Krietenbrink, J. Chem. Soc. Faraday Trans. 71 (1975) 2421.
[3] C. Binet, A. Jadi, J.C. Lavalley, J. Chim. Phys. 89 (1992) 31.
[4] A. Aboulayt, C. Binet, J.C. Lavalley, J. Chem. Soc. Faraday Trans. 91 (1995) 2913.
[5] N.N. Litchin, M. Avudaithai, Environ. Sci. Technol. 6 (1996) 2014.
[6] J. Zhuang, C.N. Rusu, J.T. Yates Jr., J. Phys. Chem. B103 (1999) 6957.
[7] V. Augugliaro, A. Bianco Prevot, J. Cáceres Vázquez, E. García López, A. Irico, V. Loddo, S. Malato Rodríguez, G. Marcì, L. Palmisano, E. Pramauro, Adv. Environ. Res., in press.
[8] V. Augugliaro, V. Loddo, M.J. López Muñoz, G. Marcì, L. Palmisano, J. Catal. 166 (1997) 272.
[9] V. Augugliaro, J. Blanco Gálvez, J. Cáceres Vázquez, E. García López, V. Loddo, M.J. López Muñoz, S. Malato, G. Marcì, L. Palmisano, M. Schiavello, J. Soria, Catal. Today 54 (1999) 245.
[10] V. Augugliaro, E. García López, V. Loddo, G. Marcì, L. Palmisano, Adv. Environ. Res. 3 (1999) 179.
[11] S.L. Murov (Ed.), Handbook of Photochemistry, Marcel Dekker, New York, 1973, p. 119.
[12] G. Spoto, C. Morterra, L. Marchese, L. Orio, A. Zecchina, Vacuum 41 (1990) 37.
[13] G. Cerrato, L. Marchese, C. Morterra, Appl. Surf. Sci. 79/71 (1993) 200.
[14] G. Busca, H. Saussey, O. Saur, J.C. Lavalley, V. Lorenzelli, Appl. Catal. 14 (1985) 245.
[15] G. Martra, Appl. Catal. A: Gen. 200 (2000) 275.
[16] M. Primet, P. Pichat, M.V. Mathieu, J. Phys. Chem. 75 (1971) 1216.
[17] C. Morterra, A. Chiorino, F. Boccuzzi, E. Fisicaro, Z. Phys. Chem. Neue Folge 124 (1981) 211.
[18] J.C. Lavalley, C. Gain, C. R. Acad. Sci. Paris 288 (1979) 177.
[19] A.G. Pelmenschikov, G. Morosi, G. Gamba, S. Coluccia, G. Martra, E.A. Paukshtis, J. Phys. Chem. 100 (1996) 5011.
[20] P. Babinec, J. Leszczynski, J. Mol. Struct. 501–502 (2000) 277.
[21] H. Celio, K. Mudalige, P. Mills, M. Trenary, Surf. Sci. 394 (1997) L168.
[22] G.S. Tyndall, J.J. Orlando, T.J. Wallington, M.D. Hurley, J. Phys. Chem. 105 (2001) 5380.
[23] K.I. Hadjiivanov, Catal. Rev. Sci. Eng. 42 (2000) 71.